Synergistic antitumor effect of the anti-ErbB2 antibodies trastuzumab and H2-18 on trastuzumab-resistant gastric cancer cells

CHAO WANG[1*], LINGFEI WANG[2*], BEIBEI LIANG[3*], BO ZHOU[4*], YU SUN[1], YANCHUN MENG[5], JIAN DONG[6], LIN CHEN[7] and BOHUA LI[8]

[1]Department of Cell Biology, Navy Medical University (The Second Military Medical University), Shanghai 200433; [2]Department of Oncology, The 903rd Hospital of The Chinese People's Liberation Army, Hangzhou, Zhejiang 310013; [3]School of Pharmacy; [4]Basic Medicine Faculty, Shanghai University of Medicine and Health Sciences, Shanghai 201318; [5]Department of Medical Oncology, Fudan University Shanghai Cancer Center, Shanghai Medical College of Fudan University, Shanghai 200032; [6]Department of Vascular Surgery, Changhai Hospital, Second Military Medical University, Shanghai 200433; [7]Department of Colorectal Surgery, Affiliated to The Department of General Surgery, Shanghai East Hospital, Tongji University School of Medicine, Shanghai 200120; [8]Shanghai Key Laboratory for Molecular Imaging, Shanghai University of Medicine and Health Sciences, Shanghai 201318, P.R. China

Received March 12, 2020; Accepted December 11, 2020

DOI: 10.3892/ol.2021.12661

Abstract. Trastuzumab resistance is a severe problem in the treatment of ErbB2-amplified cancer. Although trastuzumab plus pertuzumab is able to partly overcome trastuzumab resistance in ErbB2-overexpressing cancer, its antitumor efficacy remains limited. The present study investigated the antitumor activity of the combination of trastuzumab with H2-18, which is an antibody targetinsg ErbB2 domain I. Cell proliferation and inhibition experiments indicated that H2-18 and trastuzumab synergistically inhibited the proliferation of both the trastuzumab-sensitive gastric cancer cell line, NCI-N87 and the trastuzumab-resistant gastric cancer cell line, NCI-N87-TraRT. Furthermore, H2-18 plus trastuzumab inhibited the growth of NCI-N87-TraRT cells more effectively than trastuzumab plus pertuzumab, both *in vitro* and *in vivo*. Compared with trastuzumab plus pertuzumab, H2-18 plus trastuzumab had a potent ability to inhibit NCI-N87-TraRT cells to form colonies. Notably, H2-18 plus trastuzumab was more effective in inducing cell death than trastuzumab plus pertuzumab. The *in vivo* studies demonstrated that H2-18 plus trastuzumab effectively inhibited the growth of both NCI-N87 and NCI-N87-TraRT xenograft tumors. Further experiments revealed that in NCI-N87-TraRT cells, H2-18 plus trastuzumab was comparable to trastuzumab plus pertuzumab in the inhibition of phosphorylated (p-)HER3, p-AKT and p-ERK. However, compared with trastuzumab plus pertuzumab, H2-18 plus trastuzumab effectively activated ROS production and the phosphorylation of JNK and c-jun in NCI-N87-TraRT cells. Therefore, the superior antitumor efficacy of H2-18 plus trastuzumab over trastuzumab plus pertuzumab may be mainly attributable to the potent cell death-inducing activity. In addition, the *in vitro* and *in vivo* antitumor effect of the combination of H2-18, trastuzumab and pertuzumab were further investigated. The results revealed that H2-18 plus trastuzumab plus pertuzumab exhibited a maximal antitumor effect among all the anti-ErbB2 monoclonal antibody combinations tested. In summary, H2-18 plus trastuzumab may have potential as an effective strategy to overcome the resistance to trastuzumab in ErbB2-amplified gastric cancer cell lines.

Correspondence to: Dr Bohua Li, Shanghai Key Laboratory for Molecular Imaging, Shanghai University of Medicine and Health Sciences, 279 Zhouzhu, Pudong, Shanghai 201318, P.R. China
E-mail: bohuali1020@163.com

Dr Lin Chen, Department of Colorectal Surgery, Affiliated to The Department of General Surgery, Shanghai East Hospital, Tongji University School of Medicine, 150 JiMo Road, Pudong New Area, Shanghai 200120, P.R. China
E-mail: 896571345@qq.com

*Contributed equally

Key words: trastuzumab, H2-18, anti-ErbB2 antibody, gastric cancer, antitumor effect

Introduction

ErbB2 (or HER2) overexpression is found in 25-30% of breast cancer and 4-50% of gastric cancer cases (1-3). Trastuzumab is an anti-ErbB2 (human) antibody which is used for the clinical treatment of ErbB2-amplified metastatic breast, metastatic gastric and gastro-esophageal junction cancer (4,5). However, ~70% of patients with cancer do not respond to trastuzumab, and most of trastuzumab-responsive patients develop resistance to trastuzumab within 1 year of treatment initiation (6-8).

Despite cancer progression on ErbB2-directed therapies (9-12), ErbB2 remains considered as a valid therapeutic target. Pertuzumab is another anti-ErbB2 (human) antibody, that binds to an epitope of ErbB2 different from trastuzumab (9,13). Among the strategies to overcome trastuzumab resistance, the combination of pertuzumab and trastuzumab has provided clinical benefits (9,13). However, the objective response rate is 24.2% and the complete response rate is ~8% (9). Therefore, there is an urgent need to develop novel strategies to overcome trastuzumab resistance.

It is well established that pertuzumab recognizes domain II of ErbB2, while trastuzumab binds to domain IV. When cells are stimulated with the ErbB3 ligand, pertuzumab efficiently inhibits the formation of the ErbB2-ErbB3 complex (14), whereas the same effect is not observed with trastuzumab (14). Notably, in the absence of the ErbB3 ligand, the extent of ErbB2-ErbB3 complex formation is markedly decreased with trastuzumab treatment, whereas pertuzumab induces a very minor decrease in the formation of the ErbB2-ErbB3 complex (15). The combination of trastuzumab and pertuzumab provides a complementary mechanism of action that synergistically inhibits the proliferation of ErbB2-overexpressing breast cancer cell lines, both *in vitro* and *in vivo* (16,17). Trastuzumab predominantly interferes with ligand-independent ErbB2-ErbB3 complex formation, whereas pertuzumab inhibits ligand-induced ErbB2 heterodimerization (14,15). The clinical success of the combination of pertuzumab and trastuzumab may be partially explained by the ability to inhibit ErbB2 heterodimerization more thoroughly.

In previous studies, an ErbB2 domain I-specific human antibody, H2-18, was developed, which exhibited a more potent antitumor activity than trastuzumab and pertuzumab, either alone or in combination, in trastuzumab-resistant breast and gastric cancer cells (13,18). H2-18 functions by potently inducing programmed cell death (PCD), a different mechanism of action from either trastuzumab or pertuzumab (13,18). Therefore, it was speculated that the two anti-ErbB2 antibodies, H2-18 and trastuzumab, which have different mechanisms of action, may also achieve a synergistic effect on the inhibition of trastuzumab-resistant cancer.

In the present study, the *in vivo* and *in vitro* antitumor capability of H2-18 plus trastuzumab in the trastuzumab-sensitive gastric cancer cell line, NCI-N87, and trastuzumab-resistant gastric cancer cell line, NCI-N87-TraRT, was investigated. Additionally, the antitumor effect of H2-18 plus trastuzumab was compared with that of pertuzumab plus trastuzumab.

Materials and methods

Antibodies. The H2-18 antibody was expressed and purified using a method as previously described (19). The recombinant antibody was purified by affinity chromatography on Protein A Sepharose (GE Healthcare). The purified antibodies were analyzed via 10% SDS-PAGE under non-reducing and reducing conditions, followed by Coomassie Brilliant Blue staining. Under reducing conditions, the H2-18 antibody yielded two protein bands with a molecular mass of ~50 kDa (heavy chain) and ~25 kDa (light chain), respectively (Fig. S1). The SDS-PAGE analysis under non-reducing conditions exhibited a single band at ~150 kDa for the H2-18 antibody (Fig. S1).

The anti-ErbB2 antibodies trastuzumab and pertuzumab and the anti-CD20 antibody rituximab were expressed and purified by a similar method described in previous studies (20-22). The drug concentrations used in the present experiments and the ratio of anti-ErbB2 antibodies in antibody combinations were based on previous experiments (13,23).

Cell lines and mice. NCI-N87 is an ErbB2-amplified human gastric cancer cell line. BT-474 is an ErbB2-amplified human breast cancer cell line. All the cell lines were obtained from the American Type Culture Collection and were routinely cultured in DMEM (Thermo Fisher Scientific, Inc.) supplemented with 10% FBS (Thermo Fisher Scientific, Inc.), 100 U/ml penicillin, and 100 μg/m streptomycin (Gibco; Thermo Fisher Scientific, Inc.) at 37˚C in a humidified incubator with 5% CO_2. NCI-N87 cells were treated consecutively with trastuzumab (10 μg/ml) for 2 years to obtain a trastuzumab-resistant subline cell line, termed NCI-N87-TraRT. The cells were authenticated by morphologic and isoenzyme analyses, various times during the study period. They were routinely checked for mycoplasma contamination using Hoechst staining, which was consistently found to be negative. The BALB/c nude mice were obtained from the Shanghai Experimental Animal Center of the Chinese Academy of Sciences. The cages with food and water were changed twice a week, and the mice were fed *ad libitum*. The targeted conditions for the animal room environment and photo period were as follows: Temperature, 20-26˚C; humidity, 40-70%; light/dark cycle, 12/12 h. All the animals were treated according to the guidelines of the Committee on Animals of the Second Military Medical University (Shanghai, China). The study was approved by the Committee on Animals of the Second Military Medical University.

Detection of ErbB2 expression. BT-474, NCI-N87 and NCI-N87-TraRT cells were treated with anti-ErbB2 primary antibodies (trastuzumab, 10 μg/ml) or control anti-CD20 antibodies (rituximab, 10 μg/ml) for 1 h on ice at 4˚C. After washing 3 times, secondary goat anti-human IgG H&L (FITC) (1:100; cat. no., ab6854; Abcam) were added and incubated with cells for 40 min at 0˚C. After washing 3 times, the cells were resuspended in PBS, measured using a FACSCalibur flow cytometer (Becton, Dickinson and Company), then analyzed using FlowJo v7.6.1 software (FlowJo LLC).

Cell proliferation experiments. The cells were seeded in a 96-well plate at a density of $4x10^3$ cells/well in a humidified chamber at 37˚C with 5% CO_2. After attachment, cells were treated with control IgG (5 μg/ml), trastuzumab (5 μg/ml), pertuzumab (5 μg/ml), H2-18 (5 μg/ml), trastuzumab plus pertuzumab (5 μg/ml for both), trastuzumab plus H2-18 (5 μg/ml for both) or trastuzumab plus pertuzumab plus H2-18 (5 μg/ml for each) at 37˚C in the humidified incubator with 5% CO_2 for 5 days. The medium was changed every 2 days. Finally, the cells were incubated with Cell Counting Kit-8 (CCK-8) reagent for 60-90 min and the cell proliferation was determined according to the manufacturer's instructions (Dojindo Molecular Technologies, Inc.).

Analysis of single and combined drug effects. Cells were seeded in a 96-well plate at a density of $4x10^3$ cells/well. After attachment, the cells were treated with a range of concentrations of the aforementioned antibodies for 5 days. The media

was refreshed every 2 days. Finally, the CCK-8 assay was used to assess the cell proliferation inhibition rate. The cell proliferation inhibition rate was calculated as follows: [1-(treated cells/untreated cells)] x100%. Combination index (CI) values were calculated using the Chou-Talalay method (24). CI values <1.0 represented drug synergy, CI values=1.0 represented drug addition and CI values >1.0 indicated drug antagonism.

Reactive oxygen species (ROS) detection. The 2',7'-dichlorofluorescin diacetate (DCFH-DA; Sigma-Aldrich; Merck KGaA) was used to detect ROS. Cells were seeded in a flat-bottomed 24-well plate at a density of $1x10^5$ cells/well. After a 4-h incubation at 37˚C with control IgG (5 μg/ml), trastuzumab (5 μg/ml), pertuzumab (5 μg/ml), H2-18 (5 μg/ml), trastuzumab plus pertuzumab (5 μg/ml for both), trastuzumab plus H2-18 (5 μg/ml for both) or trastuzumab plus pertuzumab plus H2-18 (5 μg/ml for each), the cells were incubated with 10 μM DCFH-DA for 20 min at 37˚C. After washing twice with PBS, the fluorescence level of the cells treated with DCFH-DA was measured using a FACSCalibur flow cytometer (Becton, Dickinson and Company) and analyzed with FlowJo v7.6.1 software (FlowJo LLC).

Immunoblotting. Cells were seeded in a 24-well plate at a density of $1x10^5$ cells/well in a humidified atmosphere at 37˚C with 5% CO_2. After attachment, the cells were incubated with the aforementioned drugs. Subsequently, cells were lysed in RIPA buffer (25 mM Tris-HCl pH 7.6, 150 mM NaCl, 1% NP-40, 1% sodium deoxycholate and 0.1% SDS) containing a protease inhibitor cocktail (cat. no. 11836153001; Roche Diagnostics) and a phosphatase inhibitor cocktail (cat. no. P5726; Sigma-Aldrich; Merck KGaA). Protein concentrations were quantified using a BCA Protein Assay kit (cat. no. 23225; Pierce: Thermo Fisher Scientific, Inc.). Equal amounts of protein (15 μg/lane) were separated via 10% SDS-PAGE and transferred to PVDF membranes. After blocking with 5% BSA (cat. no. A1933; Sigma-Aldrich; Merck KGaA) for 1 h at 37˚C, the membranes were immunoblotted with antibodies against HER2 (cat. no. 4290s), phosphorylated (p)-HER2 (cat. no. 2243s), HER3 (cat. no. 12708s), p-HER3 (cat. no. 2842s), AKT (cat. no. 9272s), p-AKT (cat. no. 2965s), ERK1/2 (cat. no. 9102s), p-ERK1/2 (cat. no. 9106s), JNK (cat. no. 9252s), p-JNK (cat. no. 9251s), c-jun (cat. no. 9165s), p-c-jun (cat. no. 2361s), and GAPDH (1:2,000; cat. no. cat. no.5174S) (all from Cell Signaling Technology, Inc.) overnight at 4˚C. After washing with PBS-Tween 20 (0.05%), the membranes were immunoblotted with anti-rabbit IgG HRP-conjugated secondary antibody (1:3,000; cat. no. 7074s; Cell Signaling Technology, Inc.) at room temperature for 1 h. Finally, the ECL reagents (Plus-ECL; PerkinElmer, Inc.) or chemiluminescence reagents (EMD Millipore) were used to detect the proteins. Each band was quantified using TanonImage software (v1.0; Tanon Science and Technology Co., Ltd.).

Cell death assay. Cells were seeded at a density of $1x10^5$ cells/well in a flat-bottomed 24-well plate in the DMEM supplemented with 10% FBS (Thermo Fisher Scientific, Inc.), 100 U/ml penicillin, and 100 μg/ml streptomycin (Gibco; Thermo Fisher Scientific, Inc.) at 37˚C in a humidified incubator with 5% CO_2. After 24 h of attachment at 37˚C, cells were treated with control IgG (5 μg/ml), trastuzumab (5 μg/ml), pertuzumab (5 μg/ml), H2-18 (5 μg/ml), trastuzumab (5 μg/ml) plus pertuzumab (5 μg/ml), trastuzumab (5 μg/ml) plus H2-18 (5 μg/ml) and trastuzumab (5 μg/ml) plus pertuzumab (5 μg/ml) plus H2-18 (5 μg/ml). After 24 h of treatment at 37˚C, the cells were harvested and incubated with 5 μl 488-conjugated annexin-V and 0.1 μl PI (both from Tianjin Sungene Biotech Co., Ltd) per well for 15 min at room temperature. Finally, the cells were measured using a FACSCalibur flow cytometer (Becton, Dickinson and Company) and analyzed using FlowJo 7.6.1 software (FlowJo LLC).

Colony formation assay. Cells were seeded at a density of 800 cells/well in a 6-well plate. After 24 h of attachment at 37˚C, the cells were treated with control IgG (10 μg/ml), trastuzumab (10 μg/ml), pertuzumab (10 μg/ml), H2-18 (10 μg/ml), trastuzumab (10 μg/ml) plus pertuzumab (10 μg/ml), trastuzumab (10 μg/ml) plus H2-18 (10 μg/ml), and trastuzumab (10 μg/ml) plus pertuzumab (10 μg/ml) plus H2-18 (10 μg/ml) for 5 days at 37˚C. The medium was changed every 3-4 days. After 5 days of treatment, the medium was replaced with fresh RPMI 1640 medium and cultured for another 12 days at 37˚C. Finally, the colonies were fixed with 4% paraformaldehyde at room temperature for 15 min and then stained with 0.1% crystal violet at room temperature for ~10 min. The number of stained colonies containing >50 cells were recorded under a light microscope (x40).

In vivo animal experiments. NCI-N87 or NCI-N87-TraRT cells were resuspended in PBS and implanted into the right mammary fat pad of 78 6-week-old female BALB/c nude mice ($1x10^7$ cells/mouse; 78 mice in total; weight, 17-20 g; in the NCI-N87 model 7 mice per cohort, 6 cohorts in total; in the NCI-N87-TraRT model 6 mice per cohort, 6 cohorts in total). When the average volume of tumors reached 100 mm^3, the mice were randomly grouped into cohorts. The mice were injected intravenously with control IgG (10 mg/kg), trastuzumab (10 mg/kg), H2-18 (10 mg/kg), trastuzumab (10 mg/kg) plus pertuzumab (10 mg/kg), trastuzumab (10 mg/kg) plus H2-18 (10 mg/kg) and trastuzumab (10 mg/kg) plus pertuzumab (10 mg/kg) plus H2-18 (10 mg/kg), twice a week for 3 weeks. Tumors were measured with digital calipers twice a week and the volumes were calculated using the following formula: Volume (mm^3)=length x $(width)^2/2$. The duration of the experiment was 39 days. The following humane endpoints were used: Loss of significant body mass (emaciated); obvious body weight loss >20% of initial body weight; animals could not get to adequate food or water; cachexia appearance was found; and tumor volume reached ≥2,000 mm^3. All the 78 nude mice were euthanized at the end of the experiment or when they had reached these humane endpoints. The mice were sacrificed by CO_2 inhalation (with a flow rate of 30%/min).

Statistical analysis. SPSS v19.0 software (SPSS, Inc.) was used for the analysis. Normality tests were conducted before data analysis. One-way ANOVA with Tukey's multiple comparison post-hoc test was used to identify significant differences among multiple groups, unless otherwise indicated. The *in vivo*

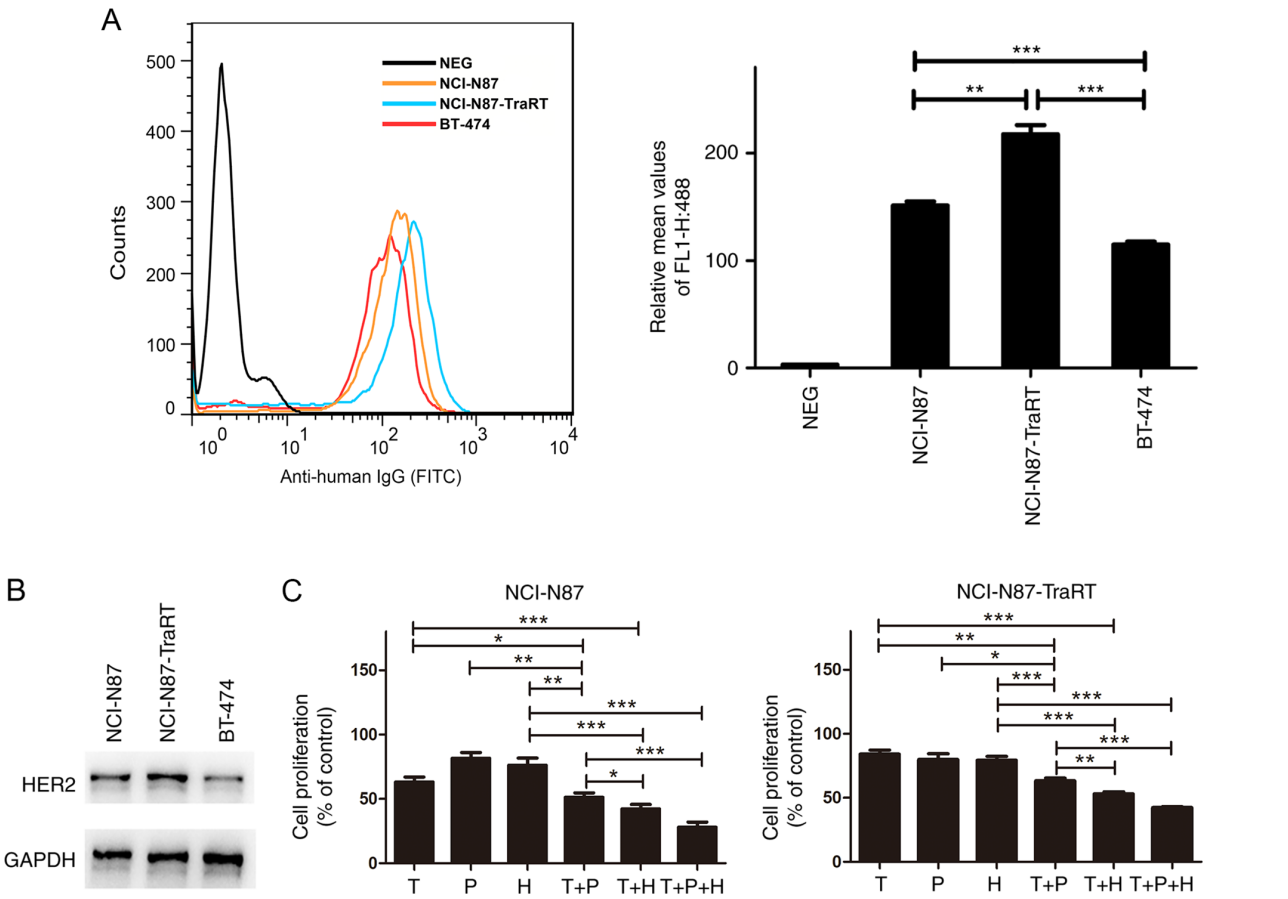

Figure 1. Addition of H2-18 to trastuzumab enhances the inhibitory effect on cell proliferation of ErbB2-overexpressing cancer cell lines. (A) Flow cytometry examining the expression levels of ErbB2 in the human gastric cancer cell lines NCI-N87 and NCI-N87-TraRT and the human breast cancer cell line, BT-474. (B) Immunoblots examining ErbB2 protein expression in NCI-N87, NCI-N87-TraRT and BT-474 cells. (C) Cell Counting Kit-8 assay was used to compare cell proliferation of the gastric cancer NCI-N87 and NCI-N87-TraRT cell lines upon the indicated treatments. *P<0.05; **P<0.01; ***P<0.001. NEG, negative control; T, trastuzumab; P, pertuzumab; H, H2-18.

animal experiments were analyzed using Kruskal-Wallis test with Dunn's post-hoc test. The data are presented as the mean ± SD (n=3). P<0.05 was considered to indicate a statistically significant difference.

Results

Addition of H2-18 to trastuzumab enhances its inhibitory effect on cell proliferation of ErbB2-overexpressing cancer cell lines. The trastuzumab-resistant cancer cell line, NCI-N87-TraRT, was derived from the trastuzumab-sensitive cancer cell line, NCI-N87 (13). It has been reported that NCI-N87 and BT-474 are high-ErbB2-expressing cell lines (25,26). Flow cytometry was used to examine ErbB2 expression in the cancer cell lines, NCI-N87, NCI-N87-TraRT and BT-474. The results revealed that ErbB2 expression in NCI-N87-TraRT cells was significantly higher compared with that in the NCI-N87 cells (Fig. 1A). Compared with that in the ErbB2-amplified BT-474 cells, NCI-N87 and NCI-N87-TraRT cells exhibited higher levels of ErbB2 receptor (Fig. 1A). The protein expression levels of ErbB2 in these cells were also confirmed using western blotting (Fig. 1B).

Subsequently, CCK-8 assays were used to determine the cell proliferation inhibitory effect of trastuzumab, pertuzumab, H2-18, trastuzumab plus pertuzumab, trastuzumab plus H2-18 and the combination of H2-18, trastuzumab and pertuzumab on NCI-N87 and NCI-N87-TraRT cells. In both ErbB2-overexpressing cancer cell lines, NCI-N87 and NCI-N87-TraRT, trastuzumab plus pertuzumab exhibited a significantly more potent inhibitory effect than trastuzumab, pertuzumab or H2-18 alone (Fig. 1C). Notably, trastuzumab plus H2-18 inhibited cell proliferation more effectively than trastuzumab plus pertuzumab (Fig. 1C). Moreover, the combination of H2-18, trastuzumab and pertuzumab exhibited the maximal inhibitory effect among all of the monoclonal antibody (mAb) combinations tested (Fig. 1C).

H2-18 and trastuzumab synergistically inhibits the cell proliferation of both trastuzumab-sensitive and trastuzumab-resistant cancer cells. The ErbB2-overexpressing trastuzumab-sensitive cancer cell line, NCI-N87, and the trastuzumab-resistant cancer cell line, NCI-N87-TraRT, were treated with various concentrations of H2-18 alone, trastuzumab alone or trastuzumab plus H2-18. The results revealed that H2-18 inhibited cell proliferation in a dose-dependent manner in both cell lines (Fig. 2A and B). The method described by Chou and Talalay was used to analyze the data. Synergy was defined as a CI value (at ED90, ED75 or ED50) <1.0, antagonism as a CI value >1.0 and additivity as a CI value of 1.0. The results demonstrated that in both cell lines, H2-18

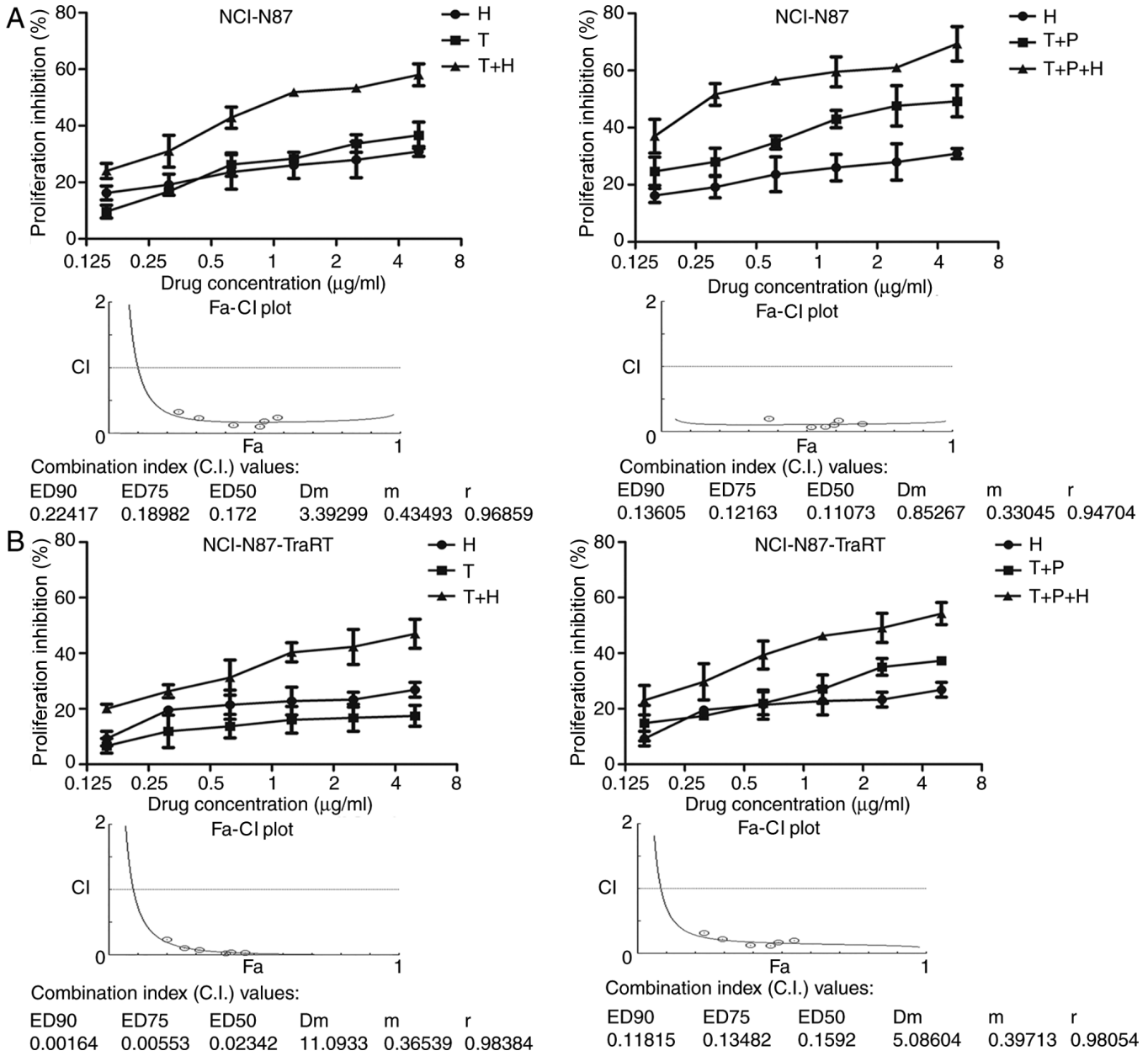

Figure 2. H2-18 and trastuzumab synergistically inhibit the proliferation of both trastuzumab-sensitive and trastuzumab-resistant cancer cells. Cell Counting Kit-8 assays were used to compare the proliferation of (A) NCI-N87 cells and (B) NCI-N87-TraRT cells upon the indicated treatments. CI values were calculated using the Chou-Talalay method. Drug synergy, addition and antagonism were defined as CI values <1.0, =1.0 or >1.0, respectively. The experiments were performed at least three times. CI, combination index; T, trastuzumab; P, pertuzumab; H, H2-18; ED, effective dose; Fa, given effect; Dm, dose of drugs that exhibit a 50% inhibition; m, slope; r, regression coefficient.

and trastuzumab inhibited the *in vitro* cell proliferation synergistically (Fig. 2A and B). In addition, NCI-N87 and NCI-N87-TraRT cells were treated with various concentrations of H2-18 alone, trastuzumab plus pertuzumab and the combination of H2-18, trastuzumab and pertuzumab. Similar results were observed (Fig. 2A and B), with the combination of H2-18 with trastuzumab plus pertuzumab synergistically inhibiting the *in vitro* proliferation of NCI-N87 and NCI-N87-TraRT cells (Fig. 2A and B).

Trastuzumab plus H2-18 exhibits a more potent inhibitory effect on colony formation compared with trastuzumab plus pertuzumab in NCI-N87-TraRT cells. In the trastuzumab-sensitive NCI-N87 cell line, trastuzumab plus H2-18 exhibited a similar inhibitory effect on the colony forming ability as that of trastuzumab plus pertuzumab; however, in trastuzumab-resistant NCI-N87-TraRT cells, trastuzumab plus H2-18 significantly decreased the formation of colonies more effectively than trastuzumab plus pertuzumab (Fig. 3). Notably, the combination of H2-18, trastuzumab and pertuzumab inhibited colony formation more potently than trastuzumab plus pertuzumab (Fig. 3).

Trastuzumab plus H2-18 exhibits a greater PCD inducing ability than trastuzumab plus pertuzumab. In both NCI-N87-TraRT and NCI-N87 cell lines, trastuzumab, pertuzumab and trastuzumab plus pertuzumab did not effectively

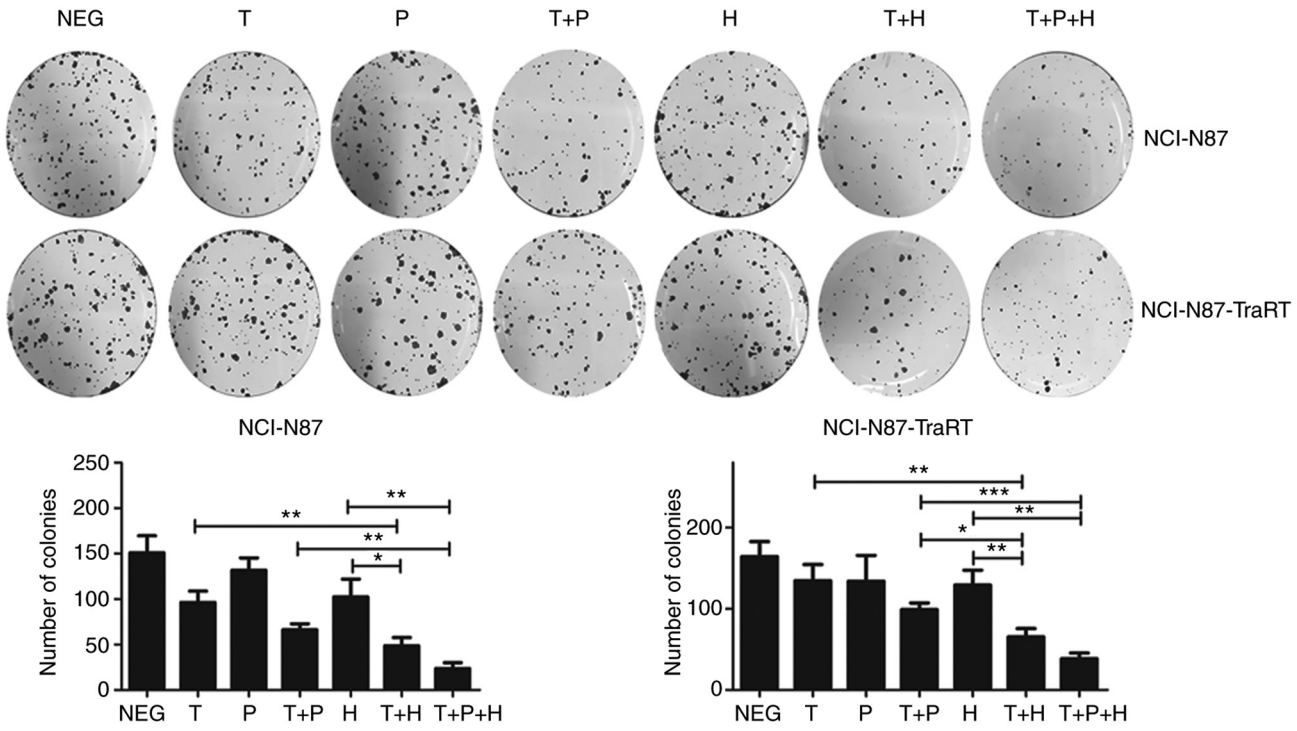

Figure 3. Trastuzumab plus H2-18 exhibits a more potent inhibitory effect on colony formation compared with trastuzumab plus pertuzumab in trastuzumab-resistant NCI-N87-TraRT cells. Representative images of colony formation assays in NCI-N87 and NCI-N87-TraRT cells with the indicated treatments are presented. The data are presented as the mean ± SD. *P<0.05; **P<0.01; ***P<0.001. NEG, negative control; T, trastuzumab; P, pertuzumab; H, H2-18.

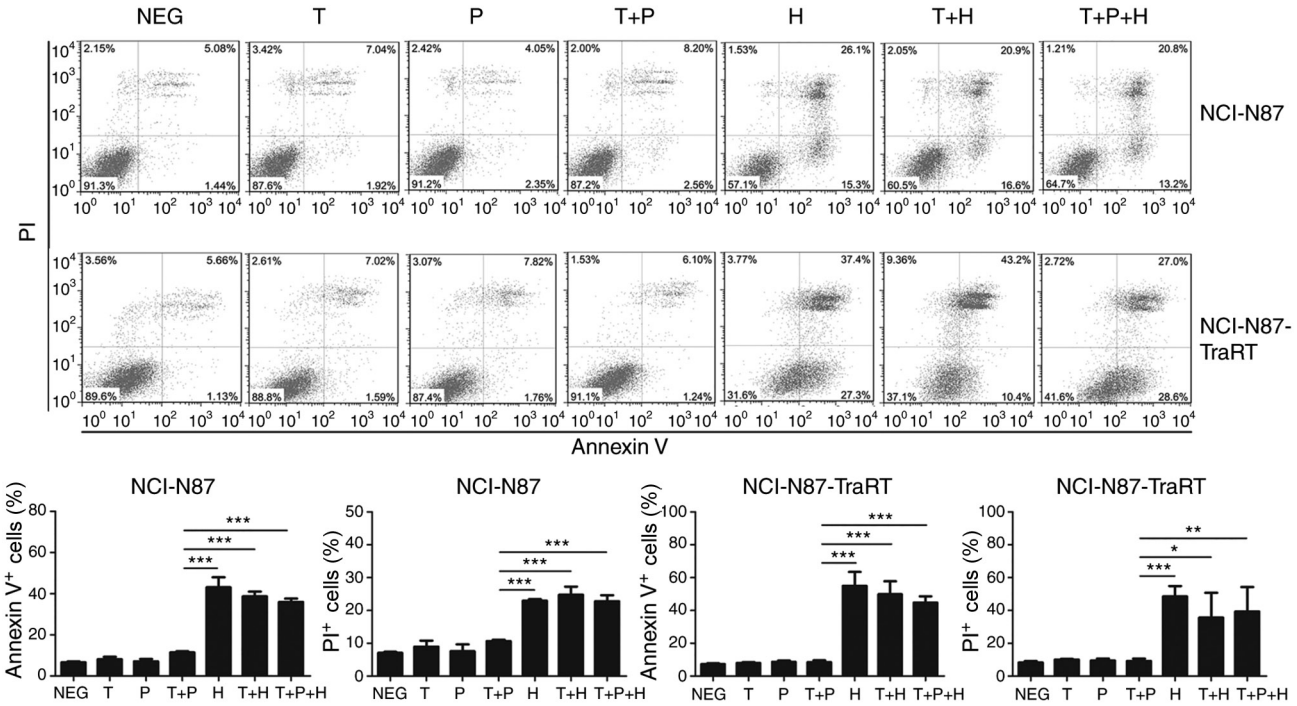

Figure 4. Trastuzumab plus H2-18 exhibits a greater programmed cell death inducing ability compared with trastuzumab plus pertuzumab. Cell death induced by trastuzumab, pertuzumab, trastuzumab plus pertuzumab, H2-18, trastuzumab plus H2-18 and trastuzumab plus pertuzumab plus H2-18 was examined by flow cytometry using an Annexin V/PI double-staining kit in the gastric cancer NCI-N87 and NCI-N87-TraRT cell lines. The data are presented as the mean ± SD. *P<0.05; **P<0.01; ***P<0.001. NEG, negative control; T, trastuzumab; P, pertuzumab; H, H2-18.

induce cell death, whereas H2-18, trastuzumab plus H2-18 and the combination of H2-18, trastuzumab and pertuzumab significantly increased cell death (Fig. 4). However, trastuzumab plus H2-18 and the combination of H2-18, trastuzumab and pertuzumab did not induce more annexin V^{+} and PI^{+} cells than H2-18 alone (Fig. 4).

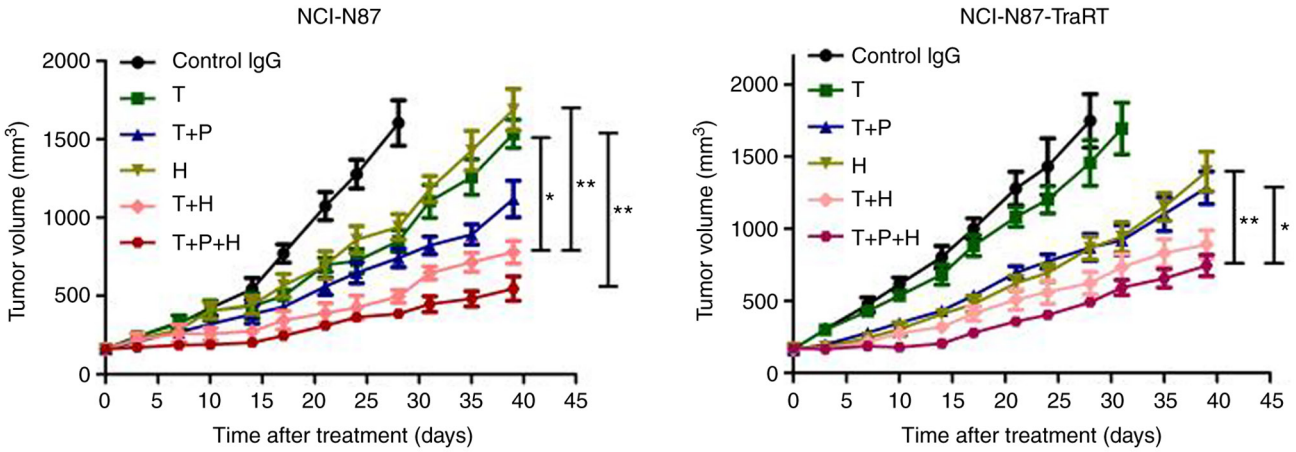

Figure 5. Trastuzumab plus H2-18 inhibits *in vivo* tumor growth more potently than trastuzumab plus pertuzumab. Tumor volume of NCI-N87 and NCI-N87-TraRT gastric tumor xenografts after treatment with control IgG (10 mg/kg, twice a week), trastuzumab (10 mg/kg, twice a week), trastuzumab (10 mg/kg, twice a week) plus pertuzumab (10 mg/kg, twice a week), H2-18 (10 mg/kg, twice a week), trastuzumab (10 mg/kg, twice a week) plus H2-18 (10 mg/kg, twice a week) and trastuzumab (10 mg/kg, twice a week) plus pertuzumab (10 mg/kg, twice a week) plus H2-18 (10 mg/kg, twice a week). The data are presented as the mean ± SEM. *P<0.05 and **P<0.01 analyzed by Kruskal-Wallis test. T, trastuzumab; P, pertuzumab; H, H2-18.

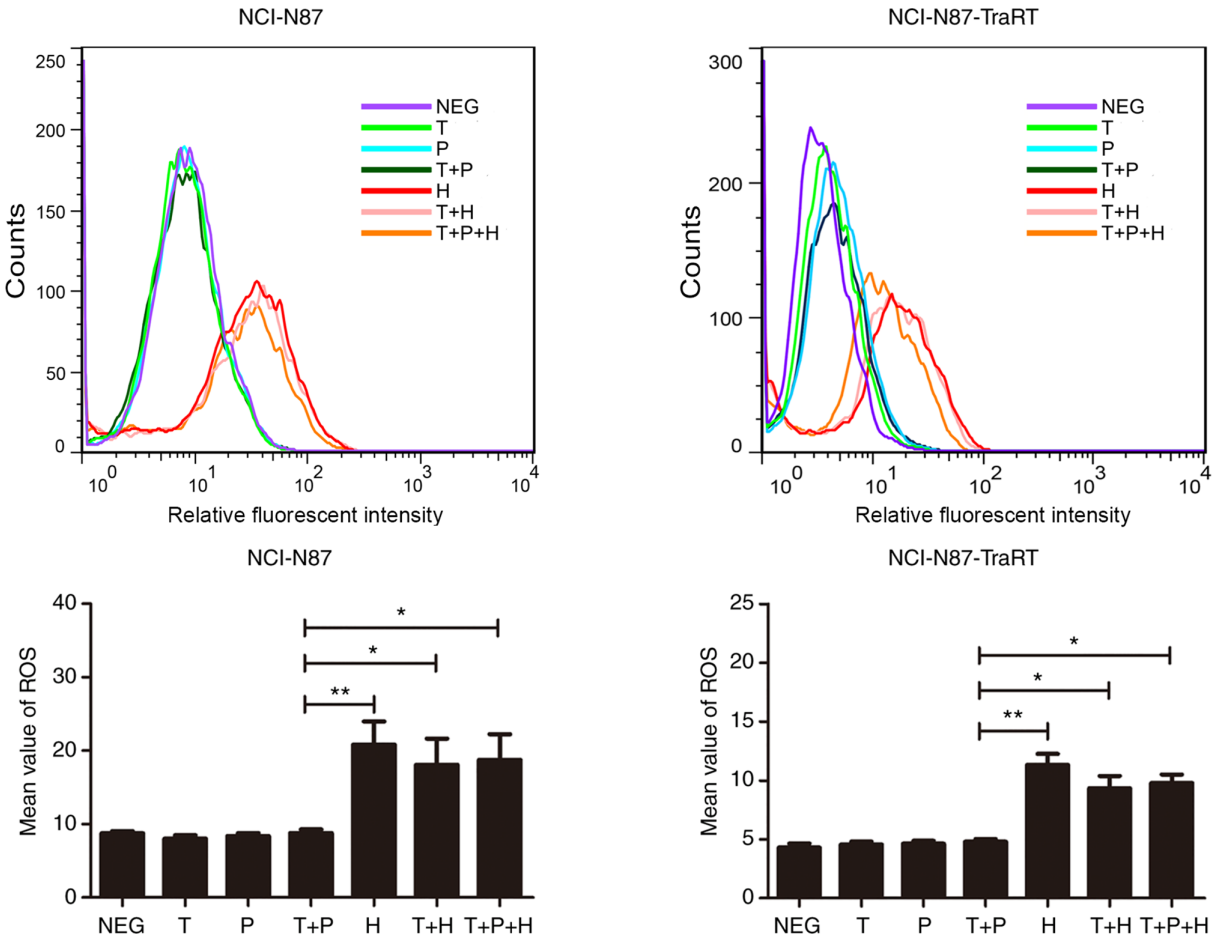

Figure 6. Trastuzumab plus H2-18 activates ROS production in both NCI-N87 and NCI-N87-TraRT cell lines. 2',7'-dichlorofluorescin diacetate was detected by flow cytometry to measure the levels of ROS production in NCI-N87 and NCI-N87-TraRT cells treated with trastuzumab, pertuzumab, trastuzumab plus pertuzumab, H2-18, trastuzumab plus H2-18 and trastuzumab plus pertuzumab plus H2-18 for 4 h. The data are presented as the mean ± SD (n=3). *P<0.05; **P<0.01. NEG, negative control; T, trastuzumab; P, pertuzumab; H, H2-18; ROS, reactive oxygen species.

Trastuzumab plus H2-18 inhibits in vivo tumor growth more potently than trastuzumab plus pertuzumab. In the NCI-N87 tumor xenografts, trastuzumab plus H2-18 exhibited a more potent inhibitory effect on tumor growth compared with that in the mice treated with trastuzumab or H2-18 alone, and the combination of H2-18, trastuzumab and pertuzumab

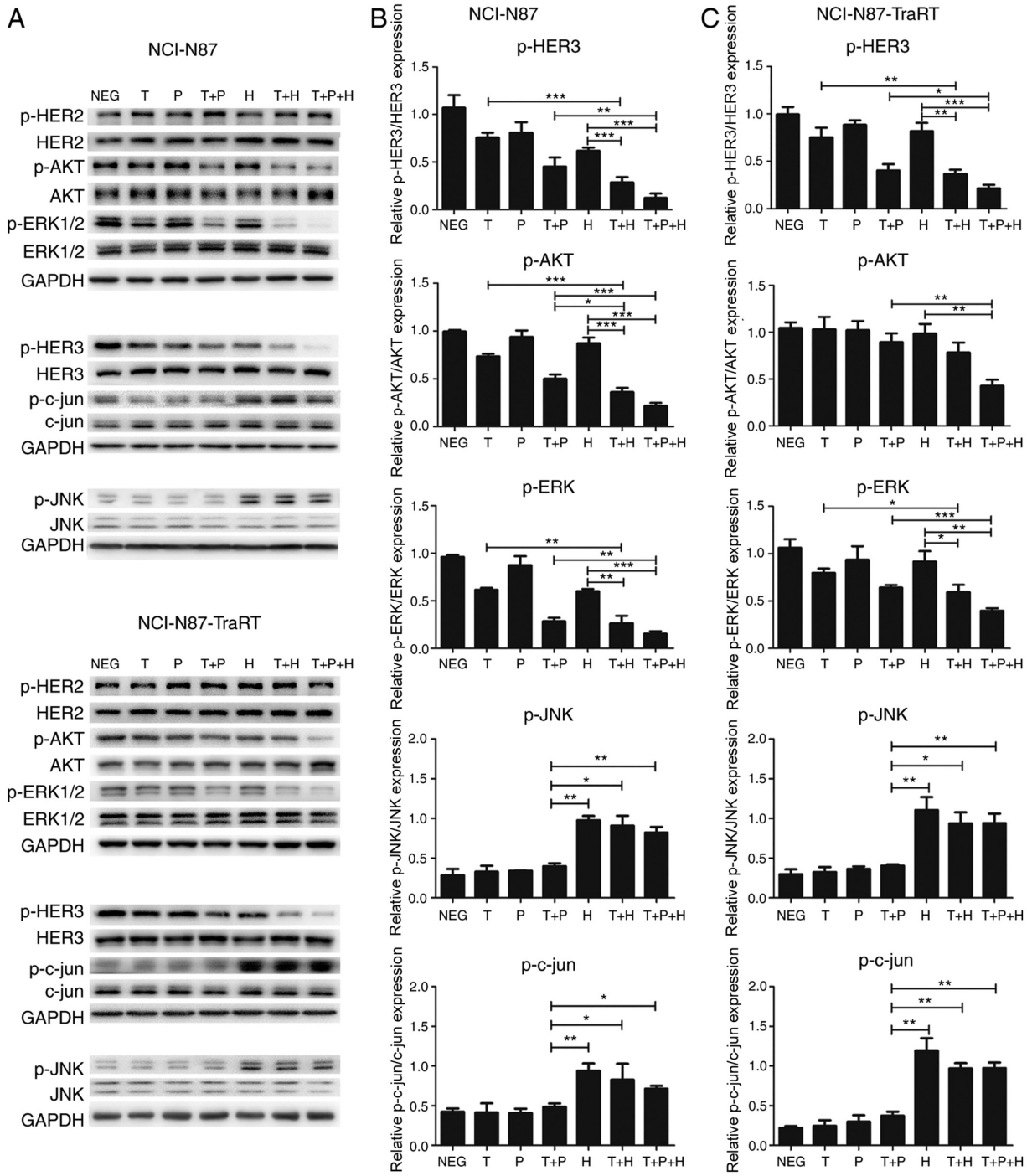

Figure 7. Trastuzumab plus H2-18 activates the ROS-JNK-c-jun signaling pathway and inhibits ErbB2 signaling pathways in both NCI-N87 and NCI-N87-TraRT cell lines. (A) Immunoblots examining the phosphorylation of HER2, HER3, AKT, ERK1/2, JNK and c-jun in NCI-N87 and NCI-N87-TraRT cells treated with trastuzumab, pertuzumab, trastuzumab plus pertuzumab, H2-18, trastuzumab plus H2-18 and trastuzumab plus pertuzumab plus H2-18 for 4 h. Quantification of the phosphorylation of HER3, AKT, ERK, JNK and c-jun in (B) NCI-N87 and (C) NCI-N87-TraRT cells following the indicated drug treatments. The data are presented as the mean ± SD. *P<0.05; **P<0.01; ***P<0.001. NEG, negative control; T, trastuzumab; P, pertuzumab; H, H2-18; p-, phosphorylated.

further augmented this inhibitory effect (Fig. 5). In the NCI-N87-TraRT tumor xenografts, trastuzumab alone did not effectively inhibit tumor growth, whereas H2-18 alone was similar to trastuzumab plus pertuzumab in terms of the inhibitory effect on tumor growth (Fig. 5). Trastuzumab plus H2-18 exhibited a more potent ability to inhibit tumor growth than trastuzumab plus pertuzumab (Fig. 5). Trastuzumab plus H2-18 and pertuzumab exhibited a more potent inhibitory effect on tumor growth compared with that in the mice treated with H2-18 and trastuzumab plus H2-18 (Fig. 5).

Trastuzumab plus H2-18 significantly induces ROS production compared with trastuzumab plus pertuzumab. In both the NCI-N87-TraRT and NCI-N87 cell lines, H2-18, trastuzumab plus H2-18 and the combination of H2-18, trastuzumab and pertuzumab significantly induced ROS production compared with that in the cells treated with

trastuzumab and pertuzumab alone and with trastuzumab plus pertuzumab (Fig. 6).

Trastuzumab plus H2-18 activates the ROS-JNK-c-jun signaling pathway in both NCI-N87 and NCI-N87-TraRT cell lines. As reported in a previous study, H2-18 induces programmed cell death through activating the RIP1-ROS-JNK-c-jun signaling pathway (18). Compared with trastuzumab plus pertuzumab, trastuzumab plus H2-18 effectively activated the phosphorylation of both JNK and c-jun in NCI-N87 cells and NCI-N87-TraRT cells (Fig. 7). The combination of H2-18, trastuzumab and pertuzumab exhibited a similar effect on the upregulation of p-JNK and p-c-jun to that of trastuzumab plus H2-18 (Fig. 7).

Trastuzumab plus H2-18 inhibits ErbB2 signaling pathways in both NCI-N87 and NCI-N87-TraRT cell lines. Western blotting was used to determine the status of ErbB2 signaling pathways in the NCI-N87 and NCI-N87-TraRT cells treated with the various mAb combinations. The results revealed that in NCI-N87 cells, all of the mAb combinations exhibited a more potent ability to inhibit the expression levels of p-HER3, p-AKT and p-ERK compared with any of the mAbs alone (Fig. 7A and B). Trastuzumab plus H2-18 inhibited p-AKT expression more effectively than trastuzumab plus pertuzumab, whereas trastuzumab plus H2-18 and trastuzumab plus pertuzumab exhibited a similar effect on the inhibition of p-HER3 and p-ERK expression (Fig. 7A and B). In the NCI-N87-TraRT cells, the ability of trastuzumab plus H2-18 to inhibit p-HER3, p-AKT and p-ERK expression was similar to that of trastuzumab plus pertuzumab (Fig. 7A and C). The combination of H2-18, trastuzumab and pertuzumab exhibited a significantly more potent effect on the inhibition of p-HER3, p-AKT and p-ERK expression compared with that in cells treated with trastuzumab plus pertuzumab in both the NCI-N87 and NCI-N87-TraRT cell lines (Fig. 7A-C). In addition, treatment with all the combinations of the mAbs or alone had no significant effect on the levels of HER2 and pHER2 (Fig. 7).

Discussion

The limited antitumor effect of trastuzumab, as well as the common occurrence of trastuzumab resistance, has driven numerous studies to develop new trastuzumab-based strategies (27,28). Previous studies have demonstrated that trastuzumab only partially inhibits ErbB2-dimer formation; ErbB2 heterodimerization may still initiate signaling events that confer resistance when ErbB2 is inhibited by trastuzumab (29,30). The combination of the two anti-ErbB2 antibodies, pertuzumab and trastuzumab, which have a complementary mechanism of action, has been reported to overcome trastuzumab resistance (9). However, the response rate of trastuzumab plus pertuzumab is currently unsatisfactory. The final results of a phase 3 study, JACOB, revealed that the addition of pertuzumab to trastuzumab for chemotherapy did not significantly improve OS in patients with $HER2^+$ metastatic gastric or gastro-oesophageal junction cancer (31,32). Therefore, further studies are required to investigate novel agents for the treatment of gastric cancer.

A trastuzumab-resistant NCI-N87-TraRT cell line derived from trastuzumab-sensitive NCI-N87 cells has been developed after two years of trastuzumab treatment (13). In the present study, the growth inhibition rate of NCI-N87-TraRT cells was very low, <20% when treated with trastuzumab, while the growth inhibition rate of the parental NCI-N87 cell line was ~40%.

An ErbB2 domain I-specific antibody, H2-18, has been previously described (18). It is well-known that trastuzumab and pertuzumab function by blocking ErbB2 dimerization and inhibiting the activation of the main downstream signaling pathways of ErbB2: PI3K/AKT and MAPK/ERK signaling pathways (19). However, neither trastuzumab nor pertuzumab significantly induced cell death in the present study. In contrast to trastuzumab and pertuzumab, H2-18 has a unique ability to overcome trastuzumab resistance both *in vitro* and *in vivo* (18). The main mechanism of action underlying the ability of H2-18 to overcome trastuzumab resistance is to induce programmed cell death through the activation of the RIP1-ROS-JNK-c-Jun signaling pathway (18). In the present study, it was found that H2-18 plus trastuzumab was more effective than pertuzumab plus trastuzumab in inhibiting cell proliferation in both the trastuzumab-sensitive NCI-N87 cells and trastuzumab-resistant NCI-N87-TraRT cells. Moreover, H2-18 and trastuzumab exhibited a synergistic antitumor effect and a more potent ability to inhibit the growth of NCI-N87-TraRT tumors than pertuzumab plus trastuzumab. Further experiments demonstrated that trastuzumab plus H2-18 decreased the formation of colonies more effectively than trastuzumab plus pertuzumab in trastuzumab-resistant NCI-N87-TraRT cells. Notably, H2-18 plus trastuzumab exhibited a more potent ability to induce cell death than pertuzumab plus trastuzumab. The expression levels of p-HER2, p-HER3, p-AKT and p-ERK in the NCI-N87-TraRT cells treated with trastuzumab plus H2-18 were similar to those in NCI-N87-TraT cells treated with trastuzumab plus pertuzumab. However, in contrast to trastuzumab plus pertuzumab, trastuzumab plus H2-18 effectively activated the phosphorylation of both JNK and c-jun in NCI-N87 cells and NCI-N87-TraRT cells. Thus, the superior antitumor efficacy of H2-18 plus trastuzumab over pertuzumab plus trastuzumab may be attributable to its enhanced ability to inhibit colony formation and to induce cell death.

In addition to H2-18 plus trastuzumab, the present study investigated the antitumor effects of the combination of H2-18, pertuzumab and trastuzumab. It is known that trastuzumab, pertuzumab and H2-18 recognize different epitopes of the ErbB2 molecule. Trastuzumab recognizes domain IV of ErbB2, while pertuzumab binds with domain II and H2-18 targets domain I. These anti-ErbB2 antibodies have different mechanisms of action on the molecule (18). The present results revealed that H2-18 plus pertuzumab plus trastuzumab provided the most potent antitumor effect compared with all of the other mAbs alone, as well as all the other combinations of mAbs, in both N87 and NCI-N87-TraRT cell lines. Therefore, the present study suggested that combination therapy of these various anti-ErbB2 antibodies may provide a novel strategy for the treatment of ErbB2-amplified cancer. However, there were several limitations in the present study, including the lack of safety and toxicity studies, the lack of further mechanistic studies and the lack of use of inhibitors of the JNK and c-jun signaling pathways. Thus, further studies are required in the future.

In summary, the present study investigated the antitumor effect of the combination of H2-18 and trastuzumab, as well as their associated mechanisms of action. The present data indicated that H2-18 plus trastuzumab exhibited a superior antitumor effect over pertuzumab plus trastuzumab in trastuzumab-resistant cancer cells. The strong antitumor efficacy of H2-18 plus trastuzumab may be attributable to a number of factors, including a more effective inhibition of colony formation and more potent induction of cell death. The present data suggested that H2-18 plus trastuzumab may have the potential to be an effective strategy to circumvent trastuzumab resistance in ErbB2-overexpressing cancer.

Acknowledgements

Not applicable.

Funding

The present study was supported by the National Natural Science Foundation of China (grant nos. 81572996, 81830052, 81573004 and 81773275), the Construction Project of Shanghai Key Laboratory of Molecular Imaging (grant no. 18DZ2260400), the Shanghai Municipal Education Commission Class II Plateau Disciplinary Construction Program of Medical Technology of Shanghai University of Medicine and Health Sciences, (2018-2020), the Shanghai Health and Family Planning Commission Foundation Youth Project (grant no. 20164Y0272), the Medical Science and Technology Project of Zhejiang Province (grant no. 2020391513), the Top-level Clinical Discipline Project of Shanghai Pudong (grant no. PWYgf2018-04) and the Pudong New District Health and Family Planning Commission Youth Science and Technology Project (grant no. PW2016B-4).

Availability of data and materials

The datasets used and/or analyzed during the current study are available from the corresponding author on reasonable request.

Authors' contributions

CW, LW and YM performed the experiments. CW, LW, BL, BZ, YS, YM, JD, LC and BL analyzed the data. LW and BL wrote the manuscript. The authenticity of data was confirmed by CW, LW and BL.All authors read and approved the final manuscript.

Ethics approval and consent to participate

All the animals were treated according to the guidelines of the Committee on Animals of the Second Military Medical University (Shanghai, China). The study was approved by the Committee on Animals of the Second Military Medical University.

Patient consent for publication

Not applicable.

Competing interests

The authors declare that they have no competing interests.

References

1. Slamon DJ, Clark GM, Wong SG, Levin WJ, Ullrich A and McGuire WL: Human breast cancer: Correlation of relapse and survival with amplification of the HER-2/neu oncogene. Science 235: 177-182, 1987.
2. Slamon DJ, Godolphin W, Jones LA, Holt JA, Wong SG, Keith DE, Levin WJ, Stuart SG, Udove J, Ullrich A and Press MF: Studies of the HER-2/neu proto-oncogene in human breast and ovarian cancer. Science 244: 707-712, 1989.
3. Thiel A and Ristimaki A: Targeted therapy in gastric cancer. APMIS 123: 365-372, 2015.
4. Bang YJ, Van Cutsem E, Feyereislova A, Chung HC, Shen L, Sawaki A, Lordick F, Ohtsu A, Omuro Y, Satoh T, *et al*: Trastuzumab in combination with chemotherapy versus chemotherapy alone for treatment of HER2-positive advanced gastric or gastro-oesophageal junction cancer (ToGA): A phase 3, open-label, randomised controlled trial. Lancet 376: 687-697, 2010.
5. Smyth EC, Verheij M, Allum W, Cunningham D, Cervantes A and Arnold D: Gastric cancer: ESMO clinical practice guidelines for diagnosis, treatment and follow-up. Ann Oncol 27: v38-v49, 2016.
6. Vogel CL, Cobleigh MA, Tripathy D, Gutheil JC, Harris LN, Fehrenbacher L, Slamon DJ, Murphy M, Novotny WF, Burchmore M, *et al*: Efficacy and safety of trastuzumab as a single agent in first-line treatment of HER2-overexpressing metastatic breast cancer. J Clin Oncol 20: 719-726, 2002.
7. Nahta R and Esteva FJ: HER2 therapy: Molecular mechanisms of trastuzumab resistance. Breast Cancer Res 8: 215, 2006.
8. Nahta R, Yu D, Hung MC, Hortobagyi GN and Esteva FJ: Mechanisms of disease: Understanding resistance to HER2-targeted therapy in human breast cancer. Nat Clin Pract Oncol 3: 269-280, 2006.
9. Baselga J, Gelmon KA, Verma S, Wardley A, Conte P, Miles D, Bianchi G, Cortes J, McNally VA, Ross GA, *et al*: Phase II trial of pertuzumab and trastuzumab in patients with human epidermal growth factor receptor 2-positive metastatic breast cancer that progressed during prior trastuzumab therapy. J Clin Oncol 28: 1138-1144, 2010.
10. Cortes J, Fumoleau P, Bianchi GV, Petrella TM, Gelmon K, Pivot X, Verma S, Albanell J, Conte P, Lluch A, *et al*: Pertuzumab monotherapy after trastuzumab-based treatment and subsequent reintroduction of trastuzumab: Activity and tolerability in patients with advanced human epidermal growth factor receptor 2-positive breast cancer. J Clin Oncol 30: 1594-1600, 2012.
11. Blackwell KL, Burstein HJ, Storniolo AM, Rugo H, Sledge G, Koehler M, Ellis C, Casey M, Vukelja S, Bischoff J, *et al*: Randomized study of Lapatinib alone or in combination with trastuzumab in women with ErbB2-positive, trastuzumab-refractory metastatic breast cancer. J Clin Oncol 28: 1124-1130, 2010.
12. von Minckwitz G, du Bois A, Schmidt M, Maass N, Cufer T, de Jongh FE, Maartense E, Zielinski C, Kaufmann M, Bauer W, *et al*: Trastuzumab beyond progression in human epidermal growth factor receptor 2-positive advanced breast cancer: A german breast group 26/breast international group 03-05 study. J Clin Oncol 27: 1999-2006, 2009.
13. Wang C, Wang L, Yu X, Zhang Y, Meng Y, Wang H, Yang Y, Gao J, Wei H, Zhao J, *et al*: Combating acquired resistance to trastuzumab by an anti-ErbB2 fully human antibody. Oncotarget 8: 42742-42751, 2017.
14. Agus DB, Akita RW, Fox WD, Lewis GD, Higgins B, Pisacane PI, Lofgren JA, Tindell C, Evans DP, Maiese K, *et al*: Targeting ligand-activated ErbB2 signaling inhibits breast and prostate tumor growth. Cancer Cell 2: 127-137, 2002.
15. Junttila TT, Akita RW, Parsons K, Fields C, Lewis Phillips GD, Friedman LS, Sampath D and Sliwkowski MX: Ligand-independent HER2/HER3/PI3K complex is disrupted by trastuzumab and is effectively inhibited by the PI3K inhibitor GDC-0941. Cancer Cell 15: 429-440, 2009.
16. Nahta R, Hung MC and Esteva FJ: The HER-2-targeting antibodies trastuzumab and pertuzumab synergistically inhibit the survival of breast cancer cells. Cancer Res 64: 2343-2346, 2004.

17. Scheuer W, Friess T, Burtscher H, Bossenmaier B, Endl J and Hasmann M: Strongly enhanced antitumor activity of trastuzumab and pertuzumab combination treatment on HER2-positive human xenograft tumor models. Cancer Res 69: 9330-9336, 2009.
18. Lu Q, Wang L, Zhang Y, Yu X, Wang C, Wang H, Yang Y, Chong X, Xia T, Meng Y, *et al*: An anti-ErbB2 fully human antibody circumvents trastuzumab resistance. Oncotarget 7: 67129-76141, 2016.
19. Li B, Meng Y, Zheng L, Zhang X, Tong Q, Tan W, Hu S, Li H, Chen Y, Song J, *et al*: Bispecific antibody to ErbB2 overcomes trastuzumab resistance through comprehensive blockade of ErbB2 heterodimerization. Cancer Res 73: 6471-6483, 2013.
20. Adams CW, Allison DE, Flagella K, Presta L, Clarke J, Dybdal N, McKeever K and Sliwkowski MX: Humanization of a recombinant monoclonal antibody to produce a therapeutic HER dimerization inhibitor, pertuzumab. Cancer Immunol Immunother 55: 717-727, 2006.
21. Li B, Shi S, Qian W, Zhao L, Zhang D, Hou S, Zheng L, Dai J, Zhao J, Wang H and Guo Y: Development of novel tetravalent anti-CD20 antibodies with potent antitumor activity. Cancer Res 68: 2400-2408, 2008.
22. Li B, Zhao L, Guo H, Wang C, Zhang X, Wu L, Chen L, Tong Q, Qian W, Wang H and Guo Y: Characterization of a rituximab variant with potent antitumor activity against rituximab-resistant B-cell lymphoma. Blood 114: 5007-5015, 2009.
23. Zhang X, Chen J, Weng Z, Li Q, Zhao L, Yu N, Deng L, Xu W, Yang Y, Zhu Z, *et al*: A new anti-HER2 antibody that enhances the anti-tumor efficacy of trastuzumab and pertuzumab with a distinct mechanism of action. Mol Immunol 119: 48-58, 2020
24. Chou TC: Drug combination studies and their synergy quantification using the Chou-Talalay method. Cancer Res 70: 440-446, 2010.
25. Yoriko YK, Sei S, Naoki H and Kaori F: Enhanced antitumor activity of trastuzumab emtansine (T-DM1) in combination with pertuzumab in a HER2-positive gastric cancer model. Oncol Rep 30: 1087-1093, 2013.
26. Stanley A, Ashrafi GH, Seddon AM and Modjtahedi H: Synergistic effects of various Her inhibitors in combination with IGF-1R, C-MET and Src targeting agents in breast cancer cell lines. Sci Rep 7: 3964, 2017.
27. Sampera A, Sánchez-Martín FJ, Arpí O, Visa L, Iglesias M, Menéndez S, Gaye É, Dalmases A, Clavé S, Gelabert-Baldrich M, *et al*: HER-family ligands promote acquired resistance to trastuzumab in gastric cancer. Mol Cancer Ther 18: 2135-2145, 2019.
28. Derakhshani A, Rezaei Z, Safarpour H, Sabri M, Mir A, Sanati MA, Vahidian F, Gholamiyan Moghadam A, Aghadoukht A, Hajiasgharzadeh K and Baradaran B: Overcoming trastuzumab resistance in HER2-positive breast cancer using combination therapy. J Cell Physiol 235: 3142-3156, 2020.
29. Ritter CA, Perez-Torres M, Rinehart C, Guix M, Dugger T, Engelman JA and Arteaga CL: Human breast cancer cells selected for resistance to trastuzumab in vivo overexpress epidermal growth factor receptor and ErbB ligands and remain dependent on the ErbB receptor network. Clin Cancer Res 13: 4909-4919, 2007.
30. Kumar R: ErbB-dependent signaling as a determinant of trastuzumab resistance. Clin Cancer Res 13: 4657-4659, 2007.
31. Shitara K, Hara H, Yoshikawa T, Fujitani K, Nishina T, Hosokawa A, Asakawa T, Kawakami S and Muro K: Pertuzumab plus trastuzumab and chemotherapy for Japanese patients with HER2-positive metastatic gastric or gastroesophageal junction cancer: A subgroup analysis of the JACOB trial. Int J Clin Oncol 25: 301-311, 2020.
32. Tabernero J, Hoff PM, Shen L, Ohtsu A, Shah MA, Cheng K, Song C, Wu H, Eng-Wong J, Kim K and Kang YK: Pertuzumab plus trastuzumab and chemotherapy for HER2-positive metastatic gastric or gastro-oesophageal junction cancer (JACOB): Final analysis of a double-blind, randomised, placebo-controlled phase 3 study. Lancet Oncol 19: 1372-1384, 2018.

This work is licensed under a Creative Commons Attribution-NonCommercial-NoDerivatives 4.0 International (CC BY-NC-ND 4.0) License.